Electronic Supplementary Material (ESI) for Lab on a Chip.

Electronic Supplementary Information (ESI)

Characterization of Fabricated Probes. Scanning electron microscope images were taken of the fabricated CF sensors to ensure uniformity and thickness of parylene encapsulation, and the structural characteristics of the exposed CF. The images were acquired with the JEOL 6010LA as detected from the collection of scattered secondary electrons with electron beam energy set to 15 kV. For all images shown, the spot size was set at 23 nm. For **Fig. 1C** and **Figs. S1C** and **D**, the magnification was set at ×370 to visualize the macroscopic features of the sensor (i.e., both the exposed sensing CF and the insulation shaft). For **Fig. 1D,** the magnification was ×7000 to reveal the boundary between the insulating parylene and the exposed CF. Other images were taken through a conventional stereo microscope with 10–45× magnification. Parylene thickness was determined from spectral reflectance measurements (Filmetrics, F-20) taken on a silicon dummy wafer stationed with the CF array wafer during parylene deposition demonstrating a film thickness of 700 nm.

16 Channel FSCV System. The 16 channel FSCV recording system comprised a laptop computer (Dell, Latitude E7450 with 16 GB memory, 2.3 GHz processor, and 64 bit Windows 7 operating system) a data acquisition card (DAQ) (National Instruments, USB-6289), an "integration circuit" box, a power supply, and current-to-voltage converting and amplification headstages. Software was written in Matlab (Mathworks, Matlab 2016a) to communicate with the DAQ to generate a clock, the voltage ramp signal that is simultaneously applied at all connected CF electrodes, and a trigger signal for activating controlled current stimulation through a separate stimulus isolator, and to acquire 16 channels of analog voltage inputs converted from the electrochemical current from the headstages. Global sampling rate was set at 25,000 samples/s, which provides an individual channel scan sampling rate of 214 samples per voltammetric scan (applied at a cycle frequency of 10 Hz). The clock was used to generate the voltage ramp (a triangular waveform from −0.3 to +1.4 to −0.3 V, for *in vivo* experiments, at a scan rate of 400 V/s for total scan duration of 8.5 ms) at the specified cycle frequency (e.g., 10 Hz). Between the 8.5 ms scans where the triangular voltage ramp was generated, the output was held at the minimum value of the voltage ramp (e.g., −0.3 V). The DAQ was configured to acquire signals in the non-referenced single-ended (NRSE) mode for the 16 input channels such that each channel was referenced to a common signal (i.e., voltage ramp), enabling analog cancellation of the applied voltage ramp that would otherwise limit dynamic range. The stimulation trigger generated a pulse for each current stimulation phase and can be configured to avoid overlap with the recording scan (in **Fig. 4A**, the trigger purposely overlaps with the scan to produce an artifact in the recording during the stimulation). The DAQ outputs the voltage ramp and stimulation trigger, and inputs 16 channels corresponding to the voltage-converted current produced by the headstage. The integration circuit relays the output ramp from the DAQ to two headstages and the electrochemical voltage signals from the headstages to the DAQ. Also, the integration circuit relays power from the voltage supply to the headstages, and provide an optional passive low pass filter to suppress quantization noise in the generated voltage ramp. The voltage supply converts mains AC power (120 V at 60 Hz in the U.S.A) to low noise DC ±12 V. Each headstage consists of 8 recording channels; each channel consists of an operational amplifier to convert and amplify current from a sensor to voltage with a gain of 4,990,000 (set by the feedback resistor), while maintaining the applied voltage at the working electrode. Two headstages can be connected to the integration box for a total of 16 recording channels. PCB layouts were sent to an external foundry (Advanced Circuits) for fabrication and then assembled in-house with off-chip circuit components (Digikey). Designs for integration circuit, power supply, and headstages, as well as software code are available online (**https://github.com/hschwerdt/multifscv**).

ESI Figures and Legends

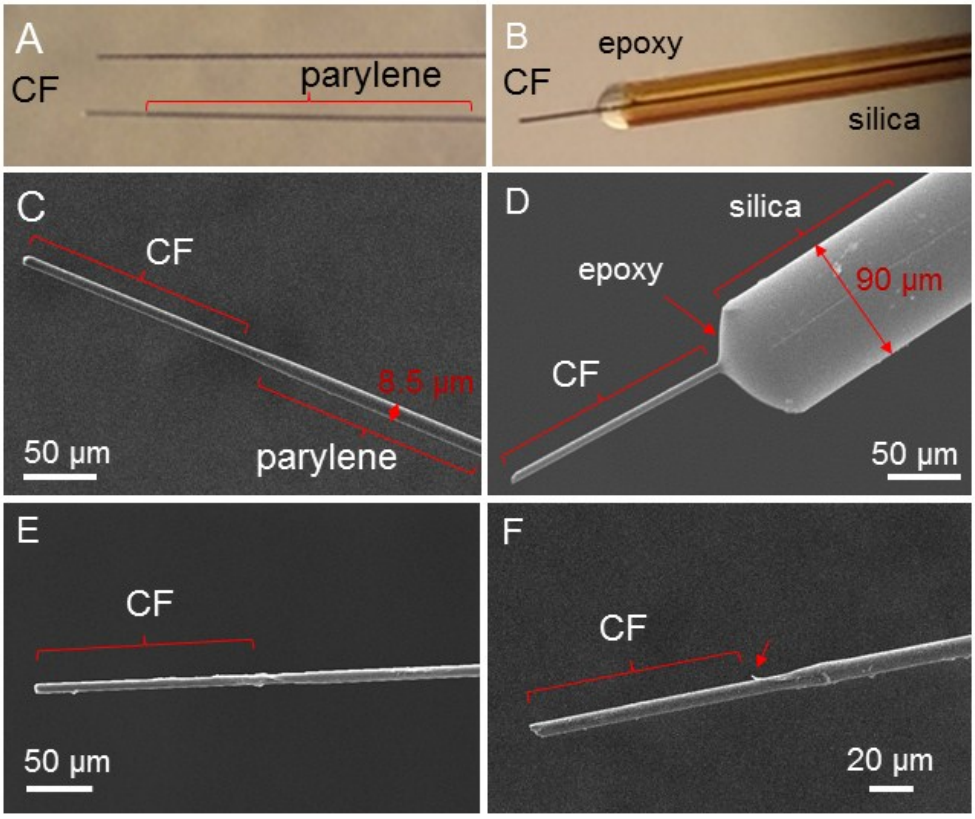

Fig. S1. Side-by-side comparison of the minimally invasive probe and the conventional CFM used for dopamine detection. (***A***) Minimally invasive probe as viewed through stereo microscope (45×). (***B***) Conventional probe as viewed through same as *A*. (***C***) Minimally invasive probe as viewed through scanning electron microscope, as fabricated with flame-etching. (***D***) Conventional probe as viewed through same as ***C***. (***E*** and ***F***) Minimally invasive probes, viewed through the same microscope as in ***C*** and ***D***, fabricated with lift-off demonstrating a less smooth transition between parylene passivation and exposed CF than with flame-etching seen in ***C***, with residual hanging parylene (arrowhead) more clearly seen in ***F***.

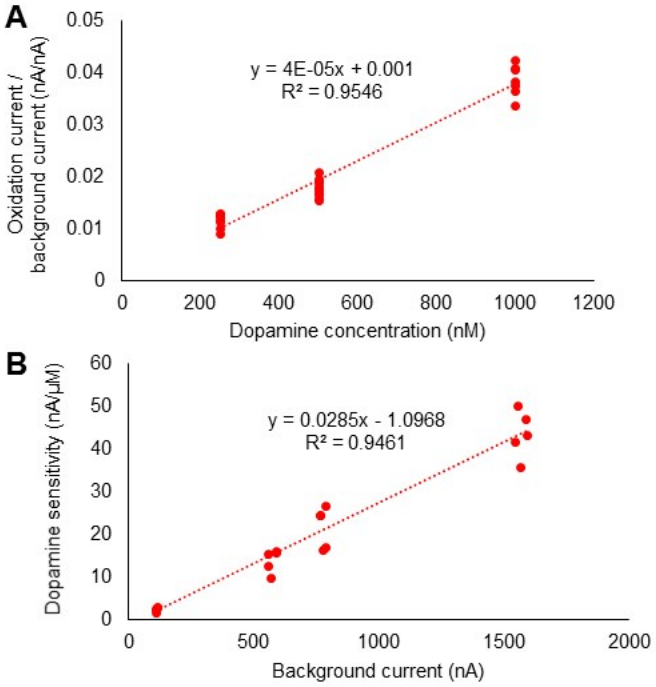

Fig. S2. In vitro dopamine measurements. (***A***) Normalized oxidation current (current at 0.6 V or the oxidation potential of dopamine divided by the background current) versus dopamine concentration. (***B***) Sensitivity of CF probe to dopamine based on the slope of generated dopamine oxidation current over concentration versus background current, displaying a linear relationship between the probe's dopamine sensitivity and its background current. The slope of this curve can be used to predict the concentration of dopamine for CF sensors exhibiting different amplitudes of background current (e.g., due to different lengths, or congruently, area of exposed CF).

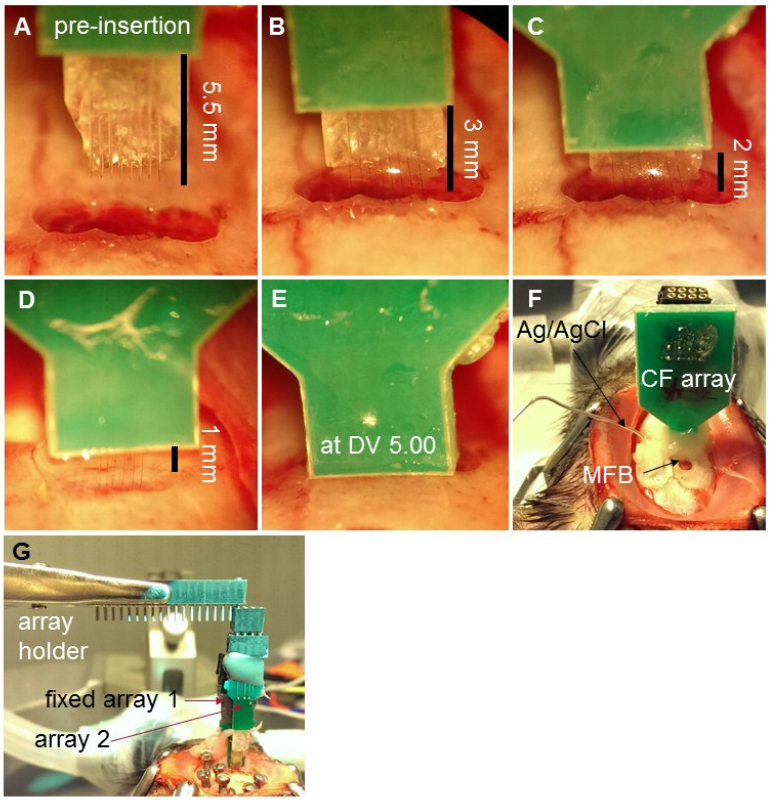

Fig. S3. Surgical implantation procedures. (***A***) The array held above targeted coordinates (AP 1.5 mm, ML 1.5–4.0 mm) and after craniotomy and dura removal. (***B***) The array lowered ~2.5 mm (3 mm portion of sensors remaining outside the brain) and apical portions of PEG inserted towards brain have dissolved. (***C***) The array lowered ~3.5 mm (2 mm of sensors remains to be implanted) and most of PEG has dissolved while the CF probes lying outside the brain remain straight. (***D***) The array lowered ~4.5 mm (1 mm of probes remain outside the brain) and all PEG dissolved. All 8 CF probes remain straight and bleeding from the brain not observed. (***E***) The array at is final depth (DV 5 mm) and CF sensing tips in the striatum brain target. (***F***) Array fixed to skull with acrylic cement along with the reference Ag/AgCl electrode in the opposite hemisphere. The craniotomy for the MFB is shown posterior to the array where the stimulating electrodes are to be lowered into. (***G***) Setup for implanting 2 arrays for measuring dopamine at 16 sites.

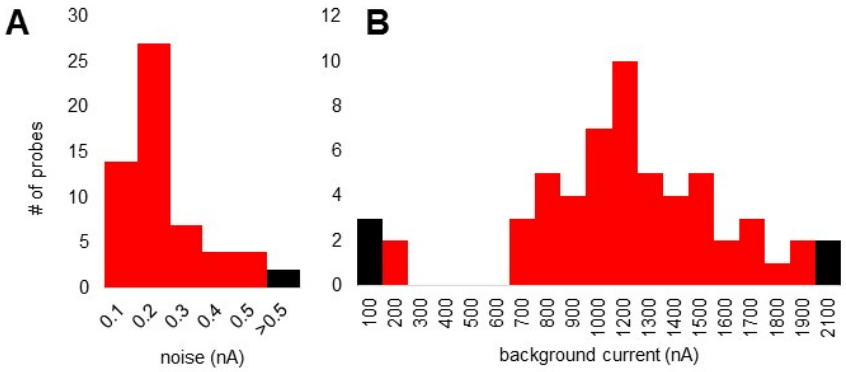

Fig. S4. Characterization of all successfully implanted probes. (***A***) Histogram of noise measured on all successfully implanted (lowered towards striatum without visible deflection) probes, delineating clusters of working (red) and non-working electrodes (black), based on described criteria for noise thresholds. (***B***) Histogram of background current measured on all implanted probes, delineating working (red) and non-working electrodes (black), based on described criteria for background current limits.

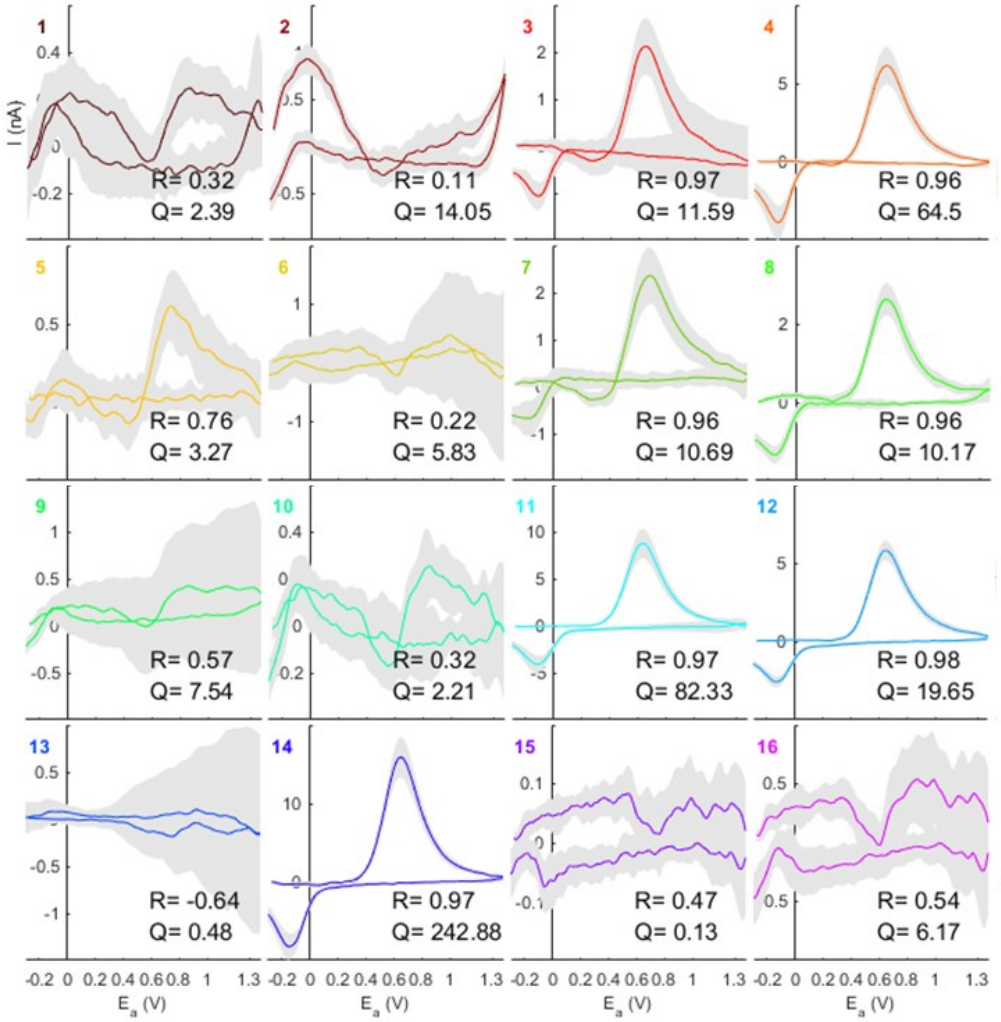

Fig. S5. Conferring dopamine chemical selectivity of the CVs (current vs. voltage plots) recorded in vivo (average of 4 stimulation-evoked dopamine measurements, post-raclopride, as shown in **Fig. 4D−G**) by correlation and PCR with in vitro CV standards (7 dopamine standards and 7 pH standards). The PCR-computed $Q\alpha$ was 585, which represents a noise tolerance level for the measurement. All measurements display a $Q < Q\alpha$, indicating that all current in the CV can be accounted for by the principle components. Pearson's correlation coefficient (R) displayed is for the dopamine standard most correlated to the in vivo measurement. It can be seen that channels 3, 4, 7, 8, 11, 12, and 14 exhibit a CV indicative of dopamine based on these guidelines. X-axes are uniform for all plots and represents applied voltage (V) during the scan. Y-axes are uniform for all plots represented measured current (nA). Gray shading represents ± standard deviation.

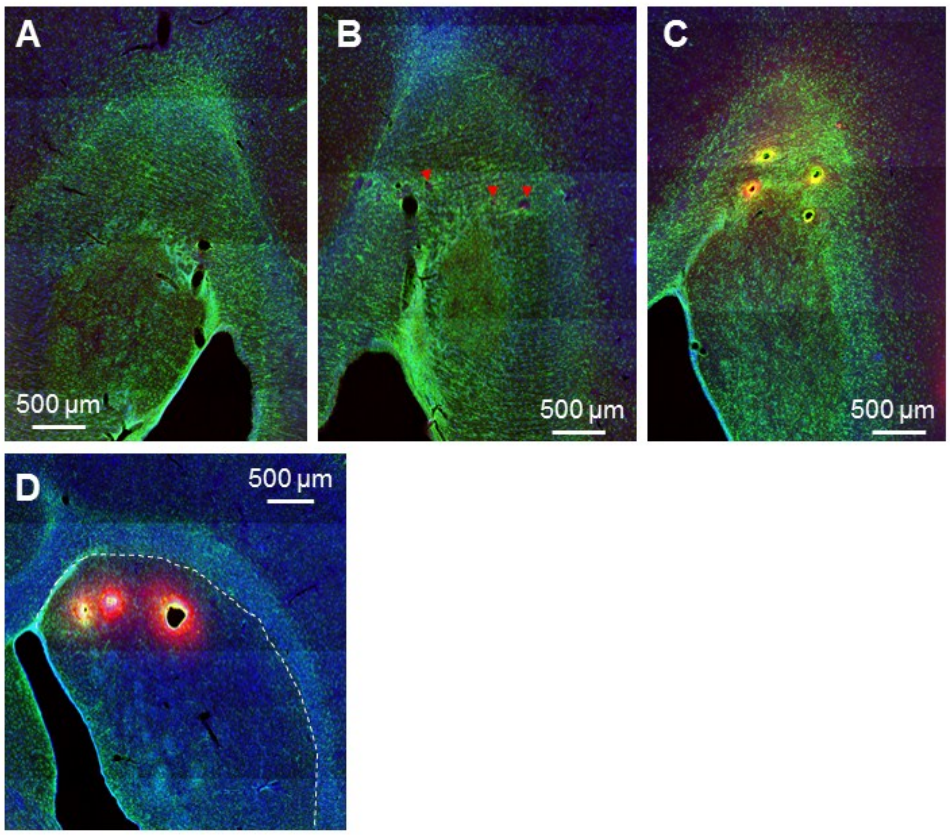

Fig. S6. Immunohistochemical analysis of horizontal brain slices for comparing longterm (> 2.5 months) inflammatory response induced by implanted probes and verifying probe recording locations by electrolytic lesion marks. Blue represents DAPI (cell nuclei), green represents GFAP (astrocytes), and red represents CD11 (microglia). (***A-C***) Expanded view of immunoreactive response of brain tissue along probe shafts dorsal to sensing tips, as shown in **Fig. 7**. (***A***) Intact, non-implanted, contralateral hemisphere of dorsal striatum (estimated DV ~3.5 mm). (***B***) Same brain slice as ***A*** on the implanted hemisphere where 8 probes were implanted into striatum. Arrow marks show putative tracks of discerned probes based on change in microglia expression intensity, which is likely produced by the electrolytic lesions made further ventral (~0.7 mm) since tracks for other non-lesioned probes are not discerned. (***C***) Corresponding slice of a separate rat implanted with conventional CFM probes (4) showing 4 clearly defined holes and increased astrocytic response around the holes as made by the probe shafts. (***D***) Slice at ~DV 4.2 mm for the same rat as in ***A*** and ***B*** where 4 sensing tips were applied with DC current to make electrolytic lesions at these positions, which can be discerned by the holes (3) generated by the lesions as well as increased microglia expression around each hole—confirming that probes had successfully reached and recorded in the striatum. Dashed curve indicates border of striatum. Channels 8, 6, 3, and 2 (descending numbers corresponding to more lateral channel sites) were applied with a DC current of 30 µA for 20–35 s. The pronounced diameter of the hole seen in the more lateral location of the striatum is likely caused by the integration of the two lesions created at channels 2 and 3, as well as the longer duration of the applied DC current (35 s) compared to more medial sites (25 s at channel 8 and 20 s at channel 6).